FARADAY

In situ and real time X-ray diffraction study of an electrocrystallisation process: Ag electrodeposition on Au(111)

Evans D. Chabala† and Trevor Rayment‡
Department of Chemistry, University of Cambridge, Lensfield Road, Cambridge, UK CB2 1EW

The electrolytic crystal growth of Ag on Au(111) under a combination of potential step and linear sweep voltammetry has been studied *in situ* and in real time with X-ray diffraction. The electrodeposition of Ag on Au(111) was an ideal system to study because the two elements have very similar lattice constants ($a = 4.09$ and 4.08 Å for Ag and Au, respectively) and hence epitaxial growth of Ag layers on Au(111) was expected. In terms of X-ray diffraction studies, the growth of an Ag ad-lattice on Au(111) led to constructive interference upon X-rays diffracted by the latter. Therefore, the differential diffracted intensity monitored at $2\theta = 38.18°$, as a function of time during electrodeposition, increased with the growth of the ad-lattice (electrodeposit). We have demonstrated how the rate of increase of the differential diffraction intensity was affected by the overpotential value stepped to, the potential sweep rate and the measurement time resolution. We conclude that under very well controlled conditions, these measurements could be used as a way of determining the rate and mode of electrolytic crystal growth.

The electrodeposition of materials at the electrode/electrolyte interface involves many stages and steps. For metal electrodeposition, the atom that ends up incorporated into the lattice of the electrodeposit is initially present as a solvated ion in the electrolyte.[1] The solvated ion has to diffuse to the electrode and be discharged before it is deposited on the electrode. After discharging, the adatom loses its solvation sheath wholly or partially. The adatom on the surface may then diffuse to a particular site to become incorporated into the ad-lattice. Alternatively, a solvated ion might be discharged, de-solvated and be transferred directly to the building site of the crystal ad-lattice.[2,3] The difficulty of studying such an electrodeposition process arises from the fact that the material transfer process from solution to the electrode and incorporation of adatoms into the ad-lattice are not easily distinguishable by methods which rely on charge-transfer measurements at the interface.[4] If it were possible to measure the growth rate of the ad-lattice during electrodeposition while controlling diffusion from solution, it might be possible to distinguish between mass transport in solution and different modes of crystal growth. In this paper, we present the new approach of using X-ray diffraction (XRD) to monitor the growth rate of the electrodeposit lattice *in situ* and in real time at the electrode/electrolyte interface.

The XRD method that we have used in this work is differential diffraction, in which the diffraction of X-rays by the substrate (electrode) is monitored during (electro-)deposition. The presence of the deposit (even just a monolayer) on the substrate (electrode) results in characteristic interference upon diffraction of X-rays by the latter.[5] It is possible to choose a system in which the material to be (electro-)deposited has a very similar lattice constant to that of the substrate (electrode) so that epitaxial growth of the former on the latter would result. In such a case, the growth of the ad-lattice (electrodeposit) will result in constructive interference upon X-rays diffracted by the substrate (electrode). Consequently, an increase in the intensity of the X-rays diffracted from the electrode–deposit system could be monitored as a measure of the growth of the ad-lattice. Since this increase in the intensity would result from the growth of the ad-lattice on the electrode, the rate of the increase of the diffracted intensity will be a direct measure of the rate of incorporation of atoms into the ad-lattice. We hope that the specific nature of the time variation of the diffracted intensity with electrodeposition can be used as a measure of the growth mode of the ad-lattice (*cf.* ref. 6). Furthermore, it should be possible to investigate the effect of additives on the rate of growth of the electrodeposit, all other conditions being the same.[6,7] It is hoped that such structural information on the growth rate/mode of the electrodeposit will be valuable in the theory and application of electrolytic crystal growth.[7]

Some preliminary results obtained with this technique are given here for the investigation of the growth rate and mode of Ag electrodeposition on Au(111).

The electrodeposition of Ag on Au(111) was done from an electrolyte solution of 1 mmol Ag^+ in an acetate solution (0.1 mol l^{-1} CH_3COOH and 0.1 mol l^{-1} CH_3COONa, Aldrich, 99.99% and 99.995%, respectively). The solutions were made with ultra pure water (18.2 MΩ, Elgastat Maxima 240, Elga Ltd.). Electrochemical control of the system was achieved with Hi-Tek DT 11005 potentiostat and a Hi-Tek PP R1 waveform generator. The design of the electrochemical cell used has been described elsewhere.[8] Thin films of gold with single crystalline (111) orientation were used as working electrodes. The single crystalline films were made by vacuum evaporation in a UTT400 UHV evaporator (Balzers Ltd) and the conditions and procedures used have been reported elsewhere.[8] A cyclic voltammogram of Ag electrodeposition on the Au(111) films in the *in situ* electrochemical cell is given in Fig. 1 for the potential range of interest. All potentials are given with respect to the Ag/Ag^+ reference couple.

The thin-film working electrode in the electrochemical cell also functioned as the sample for XRD measurements. The X-rays ($\lambda = 1.54056$ Å) incident on the back of the film (through the mica substrate on which they were grown) were diffracted by the Au(111) planes at the appropriate angle ($2\theta = 38.18°$) where the position-sensitive detector (OED-50-M, M Braun GmbH) was held fixed. On the reverse side, the thin-film working electrode was in contact with the electrolyte solution in the cell and electrochemical control of the system was maintained without interruption while diffraction measurements were made (see ref. 8). The area of the thin-film working electrode was 2.84 cm^2 and a roughness factor of 1.3 was used, as determined for evaporated films by Sieradzki and co-workers.[9]

Diffraction patterns were collected on a multichannel analyser (MCA 1/3, M Braun GmbH) and were stored in different segments of memory as a function of time at time resolutions of 2 and 0.2 s per pattern. The latter was achieved by using a counter/timer card (DT 2819, Data Translations Inc.) with digital input/output which was programmed to output an address to the MCA at the preset time resolution.

† E-mail: edc10@cus.cam.ac.uk
‡ E-mail: tr22@cus.cam.ac.uk

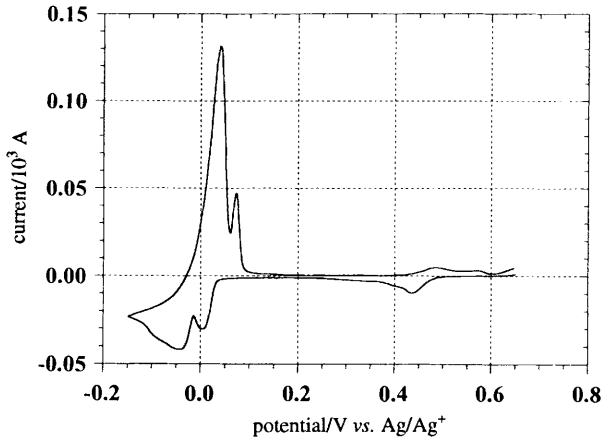

Fig. 1 Cyclic voltammogram of Ag electrodeposition on Au(111) from an acetate electrolyte (see text for details). Scan rate 10 mV s^{-1}. Two underpotential peaks are visible before bulk deposition. The potential is given with respect to the Ag/Ag^+ couple.

Further details of the data collection system have been described elsewhere.[10]

To obtain differential patterns from XRD patterns collected during the electrodeposition process, the diffraction pattern of the 'bare' electrode was subtracted from all the other patterns collected during the experiment. This experiment employed a combination of potential step and linear sweep modes, as illustrated in Fig. 2(*a*), which shows the potential as a function of time. The potential was held at 600 mV initially for 10 or 1 s (depending on the resolution) to record background diffraction patterns, and at the end of the experiment cycle, the potential was stepped back to this point and held there for 30 s in order to allow the system to relax back to initial conditions.

The potential was stepped from the background value to an overpotential value of either −50 or −70 mV and then scanned at different rates (1 mV and 10 mV s^{-1}), depending on the time resolution used, for 50 mV to a more cathodic value. This particular sequence was used in order to investigate the effect of (i) the overpotential value stepped to, (ii) the rate of potential change and (iii) the time resolution of the diffraction measurement, on the time variation of the differential diffraction intensity during electrodeposition. Fig. 2(*b*) is a 3D representation of the differential diffraction patterns obtained in the region −70 to −120 mV at a time resolution of 2 s for Ag electrodeposition on Au(111).

The deposition and desorption cycle of Ag on Au(111) was repeated about 40 times (2 s resolution) and 200 times (0.2 s resolution) to improve the signal-to-noise ratio of the diffraction patterns. It should be pointed out here that in these measurements, the detector was the limiting factor. Given a detector with better performance, it would be possible to do only a few deposition–desorption cycles to get a good signal-to-noise ratio. This would enable undesirable experimental artefacts (degradation of the electrode?) due to repeated cycling of the deposition–desorption process to be avoided.

The theory used for calculating the interference profiles in data analysis has been fully described elsewhere.[5,10,11] Fig. 3 shows the differential diffraction patterns given in Fig. 2(*b*) fitted with the calculated interference profiles. Table 1 gives the parameters obtained from fitting the experimental patterns with the calculated profiles for the 2 s resolution measurements in both overpotential regions. The significant information obtained from a fitting such as that in Fig. 3 is the spacing of the ad-layer/lattice on the substrate and the scale (size) of the differential diffraction profile. The spacing of 2.35 ± 0.05 Å (2θ = 38.18°) measured for most of the duration of the electrodeposition, as shown in Table 1, is consistent with the expected epitaxial growth of Ag on Au(111). However, spacings different from this value were also measured in the initial stages of the electrodeposition process in the case of the lower overpotential value (see Table 1). The significance of this is discussed below.

The differential diffraction peak scale was normalised so that for the background diffraction peaks collected at 600 mV, the change in intensity (ΔI) is 0, and the scales of all the other differential diffraction patterns were given as a ratio of the largest scale measured. Normalised ΔI is plotted as a function of time in Fig. 4 for the electrodeposition of Ag on Au(111) for the 2 s resolution (1 mV s^{-1}) measurement in the overpotential ranges −70 to −120 mV and −50 to −100 mV. The insert gives the charge density measured as a function of potential in terms monolayers of Ag deposited for both overpotential regions.

For the overpotential region −70 to −120 mV, the charge density variation (Fig. 4, insert) in the first 10 s (10 mV) was steeper than for the rest of the scan, while ΔI as a function of time in the same interval was not as steep (Fig. 4). Instead, the rate of increase of the differential diffraction intensity was constant in the first 20 s (20 mV). This difference in the rate of increase of charge density and differential diffraction intensity measured must be due to the fact that the former measured charge transfer at the interface while the latter measured the incorporation of material into the lattice. From these observations, it could be concluded that the rate of incorporation of Ag into the ad-lattice was slower than the rate of charge

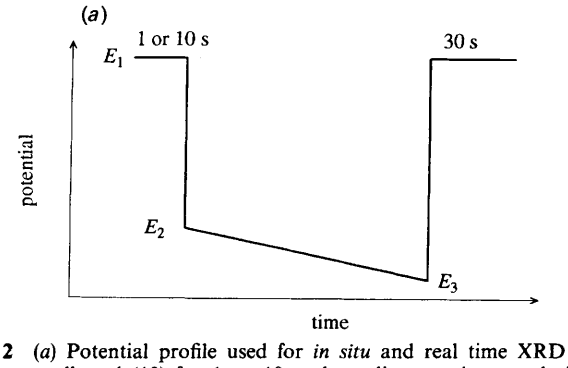

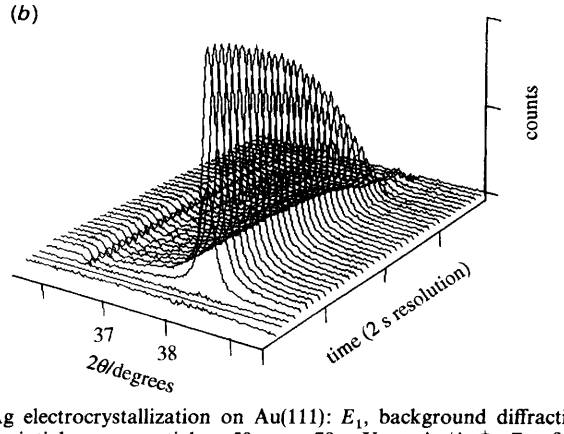

Fig. 2 (*a*) Potential profile used for *in situ* and real time XRD studies of Ag electrocrystallization on Au(111): E_1, background diffraction patterns collected (10) for 1 or 10 s, depending on time resolution used; E_2, intial overpotential, −50 or −70 mV *vs.* Ag/Ag^+; E_3, final overpotential (= E_2 + 50 mV) reached by scanning potential at 1 or 10 mV s^{-1}, depending on time resolution used. The potential was then stepped back to E_1 for 30 s to allow the system to relax back to initial conditions. (*b*) 3D representation of differential XRD patterns for the overpotential region −50 to −100 mV *vs.* Ag/Ag^+ collected using the potential profile given in (*a*). The straight line is the background pattern subtracted after stepping the potential back to the initial anodic value [E_1, see (*a*)]. Note that the differential XRD intensity falls back to zero upon stepping the potential back to E_1.

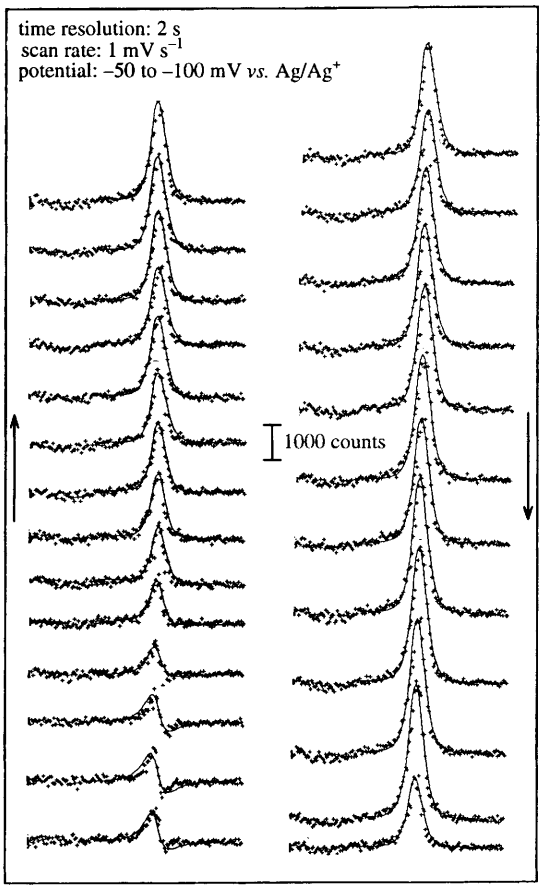

Fig. 3 The differential XRD patterns (crosses) given in Fig. 2(*b*) fitted with calculated interference profiles (solid lines) for the growth of an Ag ad-lattice on Au(111). XRD patterns were measured at $2\theta = 38.18°$. For a detailed theory of calculation of the interference profiles, see ref. 8 and 11. The arrows indicate the direction of the potential–time change. The first differential diffraction pattern corresponds to the first measurement made after stepping the potential to E_2 (−50 mV in this case).

transfer at the electrochemical interface in the first 10 s. Subsequently, after 20 s, the two rates were similar (Fig. 4, solid lines). This could indicate either that the rate of growth of the Ag electrodeposit lattice changed with time and more cathodic potential, or that the growth mode at more cathodic potential contributed differently to the measured differential intensity[2] (*cf.* ref. 12 and 13). The former is a more likely explanation taking into account the fact that the charge density and the differential diffraction intensity variation were similar at more cathodic potentials (see Fig. 4).

Considering the overpotential range −50 to −100 mV for the same scan rate and time resolution, the change in the differential intensity showed a marked discontinuity after the first 10 s before starting to increase in a stepwise pattern with time and potential scan (see Fig. 4). This discontinuity was not apparent in the charge density measured at the same time (Fig. 4, insert). The initial discontinuity in the differential intensity corresponded to spacings measured for the ad-lattice in this time interval (see Table 1) which were different from those expected for epitaxial growth of Ag on Au(111). We attribute this discontinuity in the differential diffraction intensity to (underpotential) deposition occurring before bulk deposition, and the variations in the spacings measured to possible restructuring in the ad-layer before onset of bulk deposition, as we have reported before for this system.[14] The fact that this was not observed in the first case must be due to the larger initial overpotential value used. There was another distinct discontinuity in the increase of the differential diffraction intensity at 40 s in the second overpotential region (−50

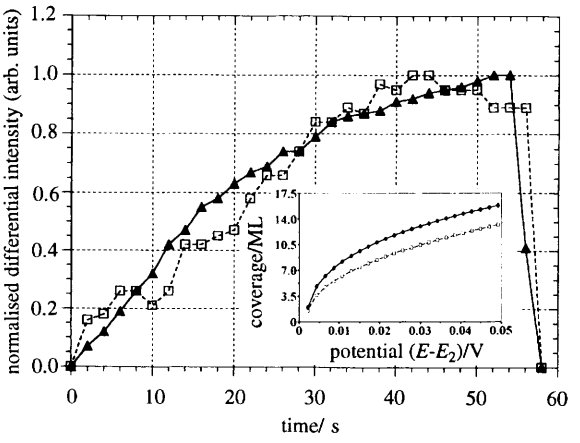

Fig. 4 Normalised differential XRD intensity (ΔI, see text) plotted against time for the 2 s resolution measurements: $E_2 = -70$ mV (triangles, solid line); $E_2 = -50$ mV (squares, dashed line). Insert: Charge density expressed as equivalent coverage (monolayers) of Ag on Au(111) as a function of potential with respect to E_2 (= −70 mV: diamonds, solid line) and (= −50 mV: squares, dashed line).

Table 1 Ad-lattice spacings and normalised differential diffraction intensity obtained from fitting differential diffraction patterns as in Fig. 3; 2 s time resolution

	spacing[a]/Å		normalised DXRD intensity	
time/s	−70 to −120 mV	−50 to −100 mV	−70 to −120 mV	−50 to −100 mV
0	bp[b]		bp[b]	
2	2.35	2.75	0.07	0.16
4	2.35	2.78	0.12	0.18
6	2.35	2.75	0.19	0.26
8	2.36	2.55	0.26	0.26
10	2.36	2.48	0.32	0.21
12	2.36	2.38	0.42	0.26
14	2.36	2.38	0.47	0.42
16	2.36	2.38	0.55	0.42
18	2.36	2.35	0.58	0.45
20	2.35	2.35	0.63	0.47
30	2.35	2.35	0.79	0.84
40	2.35	2.35	0.91	0.95
50	2.35	2.35	0.98	0.95

[a] ±0.05 Å. [b] bp, background patterns.

to −100 mV) investigated. The differential diffraction intensity stopped increasing and remained virtually constant (slight decrease) until the end of the measurement, although the charge density measured showed no such effect (*cf.* Fig. 4, insert). This again must be an indication of a change in the mode of ad-lattice growth, but more work is necessary to establish the exact cause of this effect.

Table 2 gives the spacings and normalised differential diffraction intensity for the shorter (0.2 s) time-resolved measurements. The discontinuity in the increase of the differential diffraction intensity with time in the initial stages of electrodeposition was observed in both overpotential regions investigated (see Fig. 5) and corresponded to the point at which a monolayer equivalent of charge had been passed at the interface (*cf.* Fig. 5, insert). Therefore, this discontinuity in the differential diffraction intensity is a clear demonstration of the capability of the technique used to resolve UPD, where conditions for this exist, from bulk deposit electrocrystallisation irrespective of the overpotential value stepped to, as long as a short time resolution is employed. The rate of increase of the differential diffraction intensity with time (potential) for the rest of the measurement was identical for both overpotential ranges investigated and was very similar to the rate of increase of the charge density measured with potential (Fig. 5).

Table 2 Ad-lattice spacings and normalised differential diffraction intensity obtained from fitting differential diffraction patterns for the 0.2 s time resolution measurement

	spacing[a]/Å		normalised DXRD intensity	
time/s	−70 to −120 mV	−50 to −100 mV	−70 to −120 mV	−50 to −100 mV
0	bp[b]		bp[b]	
0.2	2.58	2.65	0.28	0.25
0.4	2.65	2.65	0.28	0.28
0.6	2.70	2.75	0.26	0.22
0.8	2.55	2.75	0.21	0.24
1.0	2.45	2.75	0.31	0.28
1.2	2.40	2.55	0.40	0.41
1.4	2.38	2.45	0.47	0.41
1.6	2.35	2.45	0.50	0.51
1.8	2.35	2.35	0.53	0.63
2.0	2.35	2.35	0.61	0.62
3.0	2.35	2.35	0.76	0.74
4.0	2.35	2.35	0.94	0.91
5.0	2.35	2.35	1.0	1.0

[a] ±0.05 Å. [b] bp, background pattern.

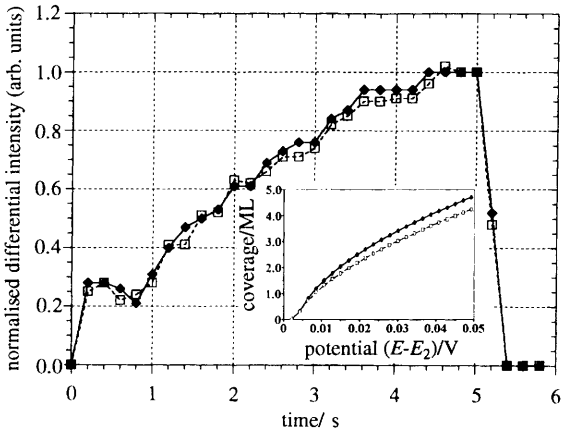

Fig. 5 ΔI plotted against time for the 0.2 s resolution measurements: $E_2 = -70$ mV (diamonds, solid line); $E_2 = -50$ mV (squares, solid line). Insert: Charge density expressed as equivalent coverage (monolayers) of Ag on Au(111) as a function of potential with respect to E_2 (= −70 mV: diamonds, solid line) and (= −50 mV: squares, dashed line).

The spacings of the adlayer measured from the first five differential diffraction patterns (in 1 s) after the potential step were between 2.45 and 2.75 ± 0.05 Å and the time interval in which they were measured corresponded to the underpotential deposition region (Fig. 5 and insert). This is more evidence for structural changes in the UPD ad-layer before bulk deposition, as has been observed before.[14] The spacing measured from differential diffraction patterns after 1.8 s was 2.35 ± 0.05 Å (see Table 2) as would be expected from an epitaxially grown Ag electrodeposit on Au(111). This spacing remained constant while the differential diffraction intensity (ΔI) increased with more electrodeposition (*cf.* Fig. 5, insert).

We have demonstrated that it is possible to use XRD to monitor electrolytic crystal growth directly *in situ* and in real time. The diffraction method used here is sensitive to the spacing of the ad-lattice on the electrode and to the quantity of material deposited. Furthermore, we have shown that the procedure we have used is sensitive to the overpotential value employed and to the time resolution of the measurement. For long time resolutions (2 s) and larger overpotentials (−70 to −120 mV), a spacing consistent with epitaxial growth of Ag on Au(111) (2.35 ± 0.05 Å) was observed throughout the duration of the measurement (*ca.* 50 s). The variations in the charge density and in the differential intensity measured with time were different at the onset of deposition, but later varied similarly. This could indicate differences between the charge transfer and electrolytic crystal growth rates of the ad-lattice at different stages (potentials) of electrodeposition.

For the lower overpotential region (−50 to −100 mV *vs.* Ag/Ag^+) with the same time resolution, it was observed that in the first 10 s, the spacing of the ad-lattice of the electrode was different from that expected for epitaxial growth (and kept varying with time), and there was a very marked discontinuity in the differential intensity with time at 8 s. This effect was attributed to UPD before bulk deposition. The differential diffraction intensity increased in a stepwise function and showed another distinct change with time after 40 s, in contrast to the variation of the charge density measured.

In the case of the shorter-time-resolved measurements, we have given further evidence for restructuring in the UPD ad-layer prior to bulk electrodeposition (Fig. 5 and Table 2), which was not apparent in current density measurements (Fig. 5, insert).

The value of being able to do measurements such as those demonstrated in this work is that under well controlled conditions (*e.g.* potentiostatic, constant charge density), quantitative comparisons of charge transfer and electrolytic crystal growth rates can be made. Furthermore, ad-lattice growth modes can be established from the time-dependent increase in the diffracted intensity.[15]

Funding from the Engineering and Physical Sciences Research Council (UK) is acknowledged for a post-doctorial research fellowship (E.D.C.) and from the Royal Society (UK) for purchase of the counter/timer board (DT2819).

References

1 B. E. Conway and J. O'M. Bockris, *Proc. R. Soc. London A*, 1958, **248**, 394.
2 M. Fleischmann and H. R. Thirsk, in *Advances in Electrochemistry and Electrochemical Engineering*, ed. P. Delahay and C. W. Tobias, Wiley, New York, 1963, vol. 3, p. 123.
3 J. A. Harrison, S. K. Rangarajan and H. R. Thirsk, *J. Electrochem. Soc.*, 1966, **113**, 1120.
4 E. Budevski, V. Bostanov and G. Staikov, *Annu. Rev. Mater. Sci.*, 1980, **10**, 85.
5 E. D. Chabala and T. Rayment, *Langmuir*, 1994, **10**, 4324.
6 R. J. Nichols, E. Bunge, H. Meyer and H. Baumgärtel, *Surf. Sci.*, 1995, **335**, 110.
7 D. Pletcher and F. C. Walsh, *Industrial Electrochemistry*, Chapman and Hall, London, 1990.
8 E. D. Chabala, H. H. Bashir, T. Rayment and M. D. Archer, *Langmuir*, 1992, **8**, 2028.
9 S. G. Corcoran, G. S. Chakarova and K. Sieradzki, *J. Electroanal. Chem.*, 1994, **377**, 85.
10 E. D. Chabala, A. R. Ramadan, T. Brunt and T. Rayment, *J. Electroanal. Chem.*, 1995, in the press.
11 T. Rayment, R. K. Thomas, G. Bonchil and J. H. White, *Mol. Phys.*, 1981, **43**, 601.
12 S. G. Corcoran, G. S. Chakarova and K. Sieradzki, *Phys. Rev. Lett.*, 1993, **71**, 1585.
13 S. G. Garcia, D. Salina, C. Mayer, J. R. Vilche, H-J. Pauling, S. Vinzelberg, G. Staikov and W. J. Lorenz, *Surf. Sci.*, 1994, **316**, 143.
14 E. D. Chabala and T. Rayment, *J. Electroanal. Chem.*, 1995, in the press.
15 R. Greef, R. Peat, L. M. Peter, D. Pletcher and J. Robinson, *Instrumental Methods in Electrochemistry*, Southampton Electrochemistry Group/Ellis Horwood, Chichester, 1985.

Communication 6/00121A; *Received 5th January*, 1996